



Synthesis and electrochemical properties of carbon nano-tubes modified spherical $\text{Li}_2\text{FeSiO}_4$ cathode material for lithium-ion batteries

Bing Huang*, Xiaodong Zheng, Mi Lu

Clean Energy Research and Development Center, Binzhou University, Binzhou, Shandong 256603, China

ARTICLE INFO

Article history:

Received 18 November 2011
Received in revised form 11 February 2012
Accepted 13 February 2012
Available online xxx

Keywords:

Lithium-ion batteries
Cathode materials
 $\text{Li}_2\text{FeSiO}_4$
Rate performance

ABSTRACT

A carbon nano-tubes (CNTs) modified spherical $\text{Li}_2\text{FeSiO}_4$ cathode material has been synthesized by a solid-state reaction method. The as-prepared $\text{Li}_2\text{FeSiO}_4$ composite has a micro-spherical morphology and is significantly constituted of a large number of nano-spheres connected by CNTs. Charge–discharge test shows that the sample exhibits discharge capacity of 153 mAh g^{-1} at 0.1 C rate in the voltage range of 1.5–4.6 V. When discharging at 10 C rate, the samples demonstrate a specific discharge capacity of 78 mAh g^{-1} . Such an enhancement of the electrochemical properties has been ascribed to a reduction of the particle size, the network-like connection with CNTs and the porous micro-spherical morphology.

© 2012 Elsevier B.V. All rights reserved.

1. Introduction

In recent years, the power system supplied to drive electric vehicles (EVs) and hybrid electric vehicles (HEVs) becomes one of hot research areas. In the light of the outstanding commercial success of the lithium-ion batteries in portable devices, they become the most promising candidate for EVs and HEVs. As a paramount component of lithium-ion batteries, cathode materials with good capacity and capacity retention at high rates are attracting vast attention [1]. After the first report from Goodenough and co-workers, LiFePO_4 has been widely studied and many achievements have been made [2,3]. As a branch of polyanion structure compounds, $\text{Li}_2\text{FeSiO}_4$ has drawn intensive attention, as it exhibits a stable cycle life with a reversible practical capacity of around 160 mAh g^{-1} [4–8]. However, the poor rate capability of $\text{Li}_2\text{FeSiO}_4$, which results from its poor intrinsic conductivity [9], inhibits its further use in large-scale battery systems.

It has been proved that reducing particles to nanometer scale can shorten the lithium ion transport distances and enhance ionic diffusion rate [10–13]. In addition, coating the particles with carbonaceous conductors [10,14–16] and doping of metallic elements [9,17–21] are effective ways to improve the electronic conductivity. These methods have been used to improve the electrochemical performance of $\text{Li}_2\text{FeSiO}_4$, individually or in combination. However, nano-sized particles easily aggregate and absorb moisture from the

air, and more binder is needed during electrode preparation due to the high specific surface of the nano-sized active material [22], all of which are disadvantageous to electrode preparation and the electrochemical properties of $\text{Li}_2\text{FeSiO}_4$.

The literature [15] reported the synthesis of $\text{Li}_2\text{FeSiO}_4$ /carbon/carbon nano-tubes by a traditional solid-state reaction method. The results indicated that the $\text{Li}_2\text{FeSiO}_4$ /C/CNT composite exhibited better electrochemical performance than the $\text{Li}_2\text{FeSiO}_4$ /C composite. It is verified that CNTs can provide valid conductive network in the electrode. Here we report on our work to improve the electrochemical properties and processability of $\text{Li}_2\text{FeSiO}_4$ materials, by making this material micro-spherical structured with a large number of primary nano-particles linked together, more importantly, CNTs and sucrose are used collaboratively to improve the electronic contact between particles. The spherical morphology may improve the process ability of the $\text{Li}_2\text{FeSiO}_4$ composite, while micro-porosity is useful for improving the wetting ability of the cathode, and network-like connections with CNTs and coated carbon for nano-sized spherical particles is good for increasing the specific surface area of the sample and the contact of particles, preventing the aggregation of ultrafine particles.

2. Experimental

$\text{Li}_2\text{FeSiO}_4$ composites were prepared by a solid-state reaction method with ball-milling and spray-drying assisted. The stoichiometric amount of $\text{FeC}_2\text{O}_4 \cdot 2\text{H}_2\text{O}$ (99.1%), $\text{Li}_2\text{C}_2\text{O}_4$ (99.9%), and SiO_2 (99.9%) was ball milled (QM-3SP04, Nanjing NanDa Instrument Plant) for 10 h in agate media in deionized water, and dried at 100°C . Then the mixtures were transferred into a tube furnace and heated to 350°C for 3 h, under an argon atmosphere. The pre-calcinated mixtures and the carbon

* Corresponding author. Tel.: +86 543 3195583; fax: +86 543 3195583.
E-mail address: huangbingzhu@sina.com (B. Huang).

precursor of sucrose (17 wt.% compared to the $\text{Li}_2\text{FeSiO}_4$) were ball milled again in ethanol for 15 h. The ball-milled mixtures were dispersed in ethanol to obtain an emulsion, then the obtained emulsion product was divided into two parts. As One part (Pr-A), 4 wt.% CNTs (the diameter is 60–70 nm and the length is 6 μm , Chengdu Organic Chemicals Co., Ltd.) compared to the $\text{Li}_2\text{FeSiO}_4$ were dispersed with the emulsion in advance, and then spray dried at 120 °C (DC1500, Shanghai Attainpak Equipment). For the sake of comparison, the other part (Pr-B) was directly spray dried. The spray dried precursors were then heated to 700 °C at a heating rate of 3 °C min⁻¹ for 10 h under an argon atmosphere. The $\text{Li}_2\text{FeSiO}_4/\text{C}/\text{CNTs}$ and $\text{Li}_2\text{FeSiO}_4/\text{C}$ samples obtained from the Pr-A and Pr-B are denoted sample-A and sample-B.

The obtained $\text{Li}_2\text{FeSiO}_4$ materials were subjected to X-ray diffraction (XRD, Panalytical X'Pert, Philips) for phase analysis using Cu K α radiation. The morphology of the spray dried precursors and $\text{Li}_2\text{FeSiO}_4$ composites were observed by scanning electron microscope (SEM, EM3200, KYKY).

For electrochemical measurements, the $\text{Li}_2\text{FeSiO}_4/\text{carbon black}/\text{polyvinylidene fluoride}$ (PVDF) mixture with weight ratio 80/10/10 for sample-A and the $\text{Li}_2\text{FeSiO}_4/\text{CNTs}/\text{carbon black}/\text{PVDF}$ mixture with weight ratio 76.8/3.2/10/10 for sample-B were used as the cathode. The amount of the CNTs is the same in both samples. The cells (CR2025 coin type) were assembled in an argon-filled glove box (Etelux). The electrolyte was 1 mol L⁻¹ LiPF₆ in ethylene carbonate/diethylene carbonate/methyl ethyl carbonate (1:1:1, v/v/v) and lithium foil was used as the counter electrode. The cells were measured using Newware galvanostatic charge–discharge unit in the voltage range of 1.5–4.6 V.

3. Results and discussion

3.1. Physical properties and morphology

Fig. 1 shows the XRD patterns of the as-prepared samples. The main diffraction peaks of both $\text{Li}_2\text{FeSiO}_4$ samples could be indexed within the orthorhombic $Pmn2_1$ space group [4,16], while the synthesized sample-B show some differences in the XRD. The major difference is the absence of the peak around 21.8–22.3° (2θ), the difference may be related to the synthesis conditions of the material such as the reducing atmosphere and sintering time [12]. Meanwhile, two unidentifiable peaks were observed in the diffractogram of sample-A and sample-B, which may be attributed to the superstructure of the synthesized composites. Meanwhile, compared with the pattern of sample-A, sample-B contains Li_2SiO_3 impurity. It is apparent that the $\text{Li}_2\text{FeSiO}_4/\text{C}/\text{CNTs}$ composite has higher crystallinity, which is similar to the result reported in literature [15].

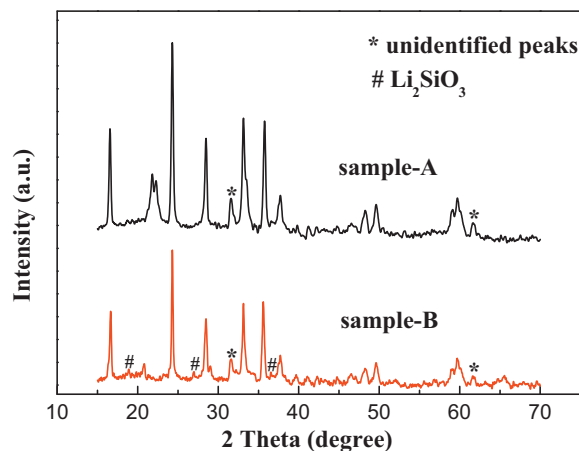


Fig. 1. XRD patterns of the sample-A and sample-B.

The XRD patterns do not show any peaks corresponding to carbon due to its low content or amorphous nature.

SEM images of precursor powders and $\text{Li}_2\text{FeSiO}_4$ samples are shown in Fig. 2a–d. The as-prepared Pr-A and Pr-B powders obtained from spray-drying exhibits sphere-like morphology, shown in Fig. 2a and b, with a particle diameter of several microns. The images indicate that the pre-calcinated mixtures, sucrose and CNTs can be bound together and micron-sized spherical particles can be obtained by spray-drying. The morphology of sample-A, obtained from the Pr-A precursor, is shown in Fig. 2c. It becomes apparent that the synthesized $\text{Li}_2\text{FeSiO}_4/\text{C}/\text{CNTs}$ sample remains spherical after calcining at 700 °C and is significantly constituted of a large number of spherical primary nano-particles. More importantly, the ultrafine primary particles were connected by the CNT networks. However, as shown in Fig. 2d, the morphology of the calcinated powders of sample-B, obtained from the Pr-B precursor, are not micro-spherical and some primary particles agglomerated with irregular morphology after calcining at 700 °C, which differs from the sample-A. Such a morphological change took place during

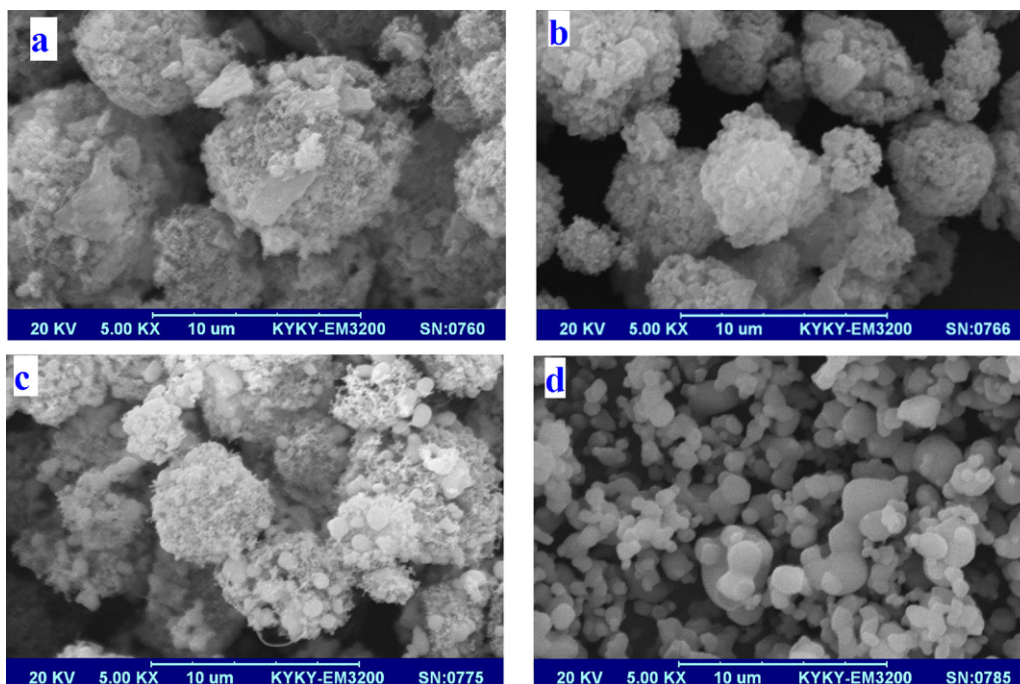


Fig. 2. SEM images of precursor powders and $\text{Li}_2\text{FeSiO}_4$ samples: (a), Pr-A; (b), Pr-B; (c), sample-A; (d), sample-B.

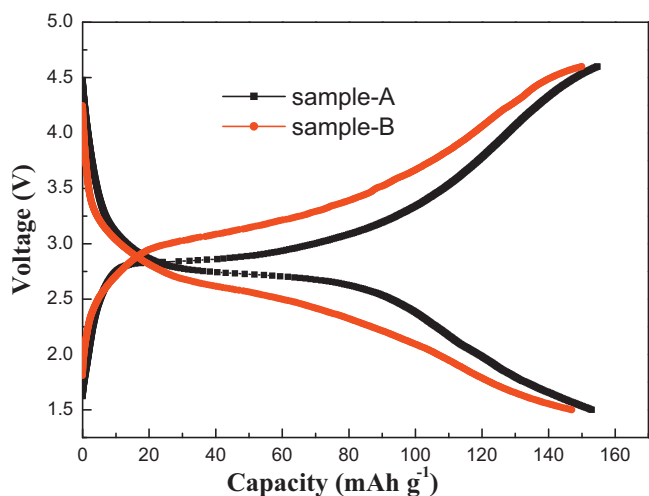


Fig. 3. Charge–discharge profiles of the $\text{Li}_2\text{FeSiO}_4$ electrode at 0.1 C rate in the voltage range of 1.5–4.6 V.

calcining. The presence of CNTs is important to keep all reactants in good contact with each other throughout the reaction and prevent the growth and agglomeration of particles. The small particle size of $\text{Li}_2\text{FeSiO}_4$ provides short pathways for rapid lithium ion and electron conduction within the nano-particles, while the coated carbon and CNTs connect the nano-particles together, providing a highly conductive channel for the electron mobility between adjacent $\text{Li}_2\text{FeSiO}_4$ nano-particles.

3.2. Electrochemical performance

Fig. 3 displays the charge–discharge behavior for the third cycle of the $\text{Li}_2\text{FeSiO}_4$ electrodes between 1.5 V and 4.6 V operating at 0.1 C rate ($C = 160 \text{ mA g}^{-1}$). The discharge capacity of the sample-A and B is 153 mAh g^{-1} and 147 mAh g^{-1} respectively. The discharge capacity of the sample-A is 3.9% higher than that of the sample-B. The potential difference between the charge and discharge plateau potentials is often used to examine the electrochemical reversibility of an electrode material. The results also show that sample-A has a smaller difference between the charge and discharge plateau potentials than that of the sample-B, which may indicate a higher electrode reaction reversibility and lower polarization for sample-A composite.

To further clarify the charge–discharge characteristics of $\text{Li}_2\text{FeSiO}_4$, the differential capacities (dQ/dV) for the third charging–discharging cycle were calculated and dQ/dV vs. voltage curves are plotted in Fig. 4, which can provide similar information of cyclic voltammograms. The oxidation/reduction peaks in the curves correspond to the charge–discharge plateaus in the charge–discharge curves [4]. As shown in Fig. 4, only a pair of redox peaks is observed for each sample, which corresponds to the lithium deintercalation and intercalation process. The redox peaks of sample-A are sharper than those of sample-B, due to more flat voltage plateaus in the charge–discharge curves for sample-A, which is in good agreement with the charge–discharge behavior in Fig. 3.

The discharge capacities of as synthesized samples at various current densities are shown in Fig. 5. The cells were charged to 4.6 V at 0.1 C rate, then discharged to 1.5 V at n C rate (where $n = 1, 3, 5, 10$). In all cases, the discharge capacity and voltage plateaus of sample-A are higher than that of sample-B. The difference between the discharge capacity of sample-A and sample-B increases with increasing current density. When the current density is as high as 10 C, the discharge capacity of sample-A is 78 mAh g^{-1} and that of

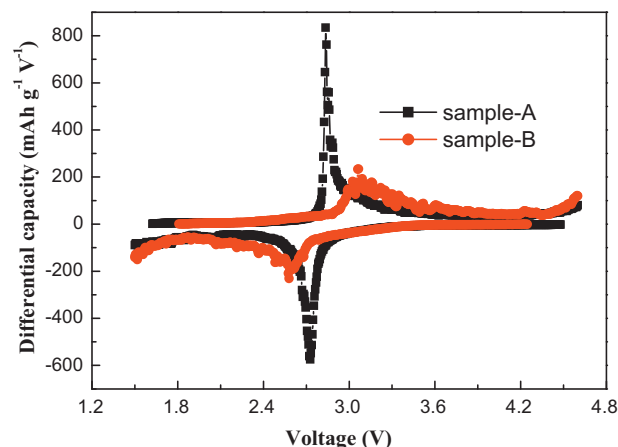


Fig. 4. Differential capacity curves of the $\text{Li}_2\text{FeSiO}_4$ electrode at 0.1 C rate in the voltage range of 1.5–4.6 V.

sample-B is only 31 mAh g^{-1} . The results show that sample-A had a much better rate performance than that of sample-B.

The cycling stability and coulombic efficiency of the $\text{Li}/\text{Li}_2\text{FeSiO}_4$ cell at various discharging rates from 0.1 to 10 C in every eight cycles are shown in Fig. 6a and b. For accurate comparison of the rate performance during discharging, the samples were charged at fixed rate of 0.1 C. The cutoff voltages were 1.5 and 4.6 V. The results indicate that following the 80 cycles sample-A and sample-B retain 97.5% and 94.8% of the original specific capacity, respectively, and the sample-A showed better capacity retention. Meanwhile, the cycle coulombic efficiency of both samples remains more than 99% from the 4th cycle to the 80th cycle.

The improved rate performance and cyclability of the sample-A can be attributed to the effects of porous micro-spherical structure and nano-sized spherical primary particles connected by the CNT networks. The network-like connection with carbon and CNTs is favorable to the electron transfer. The nano-sized spherical particle is good for increasing the area for electrode reaction and shortening the diffusion path of lithium ion. The porosity of the micro-spheres is useful for improving the wetting ability of the cathode. These can lower the electrode polarization during charge and discharge, and, thus, increase the utilization of active material, especially at high rates.

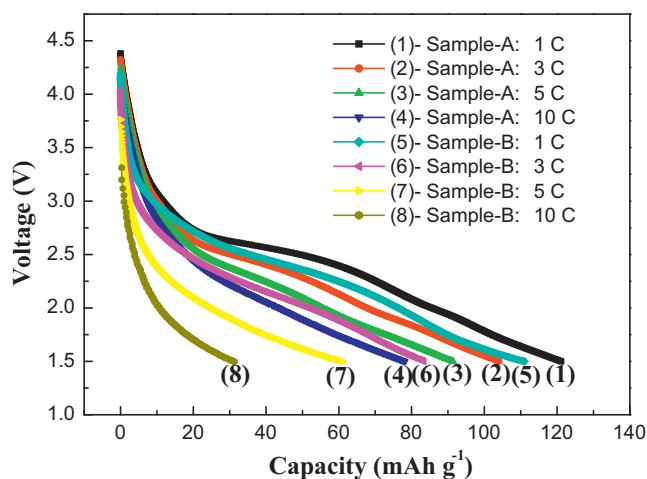


Fig. 5. Discharge curves of $\text{Li}_2\text{FeSiO}_4$ electrode at various rates.

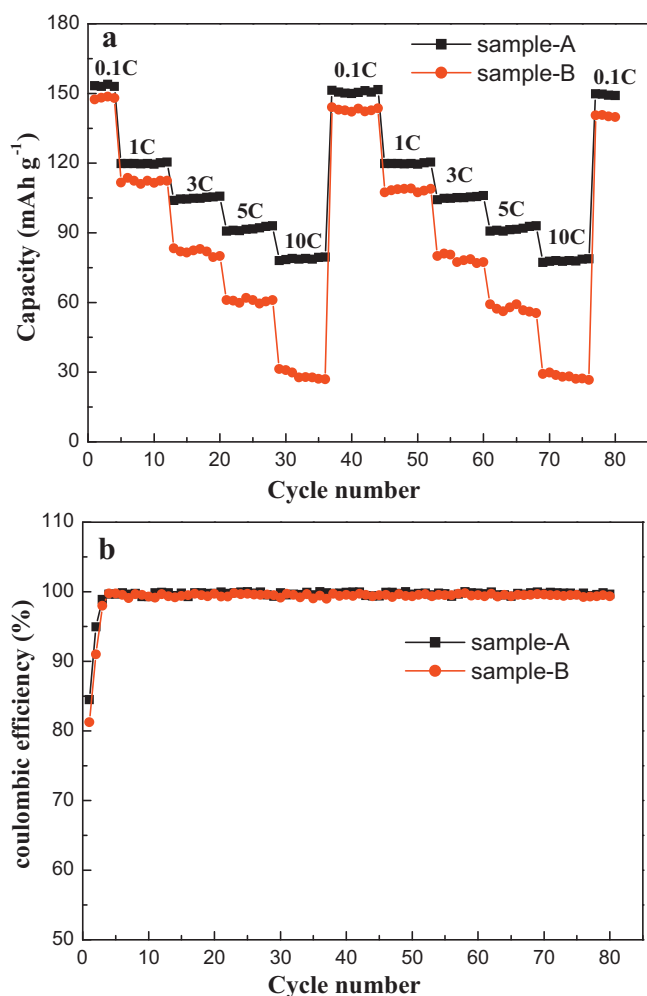


Fig. 6. Cycling stability curves (a) and coulombic efficiency curves (b) of $\text{Li}_2\text{FeSiO}_4$ composites discharging at various rates from 0.1 to 10C in every eight cycles.

4. Conclusions

In summary, we have successfully synthesized novel CNTs modified micro-spherical $\text{Li}_2\text{FeSiO}_4$ composite. The synthesized

micro-spheres contain large amount of nano-spherical primary particles connected with carbon and CNTs. The nano-spheres provide short pathways for rapid lithium ion and electronic conduction, and the carbon coating and CNTs linking improve the electronic conductivity. The results indicate that the electrochemical performance of $\text{Li}_2\text{FeSiO}_4/\text{C}/\text{CNT}$ was improved. The prepared composite is the promising material proposed as a cathode for powerful and large lithium-ion batteries.

Acknowledgments

This work was supported by Doctoral Fund of Shandong Province (BS2009NJ001), the Project of Higher Educational Science and Technology Program of Shandong Province (J10LB56).

References

- [1] M. Armand, J.M. Tarascon, *Nature* 451 (2008) 652.
- [2] A.K. Padhi, K.S. Nanjundaswamy, J.B. Goodenough, *J. Electrochem. Soc.* 144 (1997) 1188.
- [3] B. Kang, G. Ceder, *Nature* 458 (2009) 190.
- [4] A. Nytén, A. Abouimrane, M. Armand, T. Gustafsson, J.O. Thomas, *Electrochem. Commun.* 7 (2005) 156.
- [5] P. Larsson, R. Ahuja, A. Nytén, J.O. Thomas, *Electrochem. Commun.* 8 (2006) 797.
- [6] M.E. Arroyo, J.M. Amores, J.G. Martínez, E. Morán, J.M. Tarascon, M. Armand, *Solid State Ionics* 170 (2008) 1758.
- [7] S. Nishimura, S. Hayase, R. Kanno, M. Yashima, N. Nakayama, A. Yamada, *J. Am. Chem. Soc.* 130 (2008) 13212.
- [8] K. Karthikeyan, V. Aravindan, S.B. Lee, I.C. Jang, H.H. Lim, G.J. Park, M. Yoshio, Y.S. Lee, *J. Alloys Compd.* 504 (2010) 224.
- [9] R. Dominko, *J. Power Sources* 184 (2008) 462.
- [10] T. Muraliganth, K.R. Stroukoff, A. Manthiram, *Chem. Mater.* 22 (2010) 5754.
- [11] S. Zhang, C. Deng, S.Y. Yang, *Electrochem. Solid-State Lett.* 12 (2009) A136.
- [12] K.C. Kam, T. Gustafsson, J.O. Thomas, *Solid State Ionics* 192 (2011) 356.
- [13] Z.L. Gong, Y.X. Li, G.N. He, J. Li, Y. Yang, *Electrochem. Solid-State Lett.* 11 (2008) A60.
- [14] X. Huang, X. Li, H. Wang, Z. Pan, M. Qu, Z. Yu, *Solid State Ionics* 181 (2010) 1451.
- [15] X. Huang, X. Li, H. Wang, Z. Pan, M. Qu, Z. Yu, *Electrochim. Acta* 55 (2010) 7362.
- [16] R. Dominko, D.E. Conte, D. Hanzel, M. Gaberscek, J. Jamnik, *J. Power Sources* 178 (2008) 842.
- [17] S. Zhang, C. Deng, B.L. Fu, S.Y. Yang, L. Ma, *J. Electroanal. Chem.* 644 (2010) 150.
- [18] S. Zhang, C. Deng, B.L. Fu, S.Y. Yang, L. Ma, *Electrochim. Acta* 55 (2010) 8482.
- [19] C. Deng, S. Zhang, S.Y. Yang, *J. Alloys Compd.* 487 (2009) L18.
- [20] L.M. Li, H.J. Guo, X.H. Li, Z.X. Wang, W.J. Peng, K.X. Xiang, X. Cao, *J. Power Sources* 189 (2009) 45.
- [21] H. Guo, X. Cao, X. Li, L. Li, X. Li, Z. Wang, W. Peng, Q. Li, *Electrochim. Acta* 55 (2010) 8036.
- [22] B. Huang, X. Fan, X. Zheng, M. Lu, *J. Alloys Compd.* 509 (2011) 4765.